Inorganica Chimica Acta 387 (2012) 346–351

Contents lists available at SciVerse ScienceDirect

Inorganica Chimica Acta

journal homepage: www.elsevier.com/locate/ica

Synthesis, crystal structures, and deprotonation of *cis*- and *trans*-octahedral nickel(II) complexes with a 14-membered tetraaza macrocycle bearing two *N*-phenacyl pendant arms

Hyunja Kim [a], Shin-Geol Kang [a,*], Chee-Hun Kwak [b]

[a] Department of Chemistry, Daegu University, Gyeongsan 712-714, Republic of Korea
[b] Department of Chemistry, Sunchon National University, Sunchon 540-742, Republic of Korea

ARTICLE INFO

Article history:
Received 13 October 2011
Received in revised form 7 February 2012
Accepted 15 February 2012
Available online 1 March 2012

Keywords:
Macrocyclic compounds
Geometric isomers
Functional pendant arms
Tautomerism
N-Phenacyl groups
Deprotonation

ABSTRACT

The di-*N*-functionalized macrocycle 2,13-bis(2-phenacyl)-5,16-dimethyl-2,6,13,17-tetraazatricyclo$[16.4.0.^{1.18}0^{7.12}]$docosane (H_2L^2) bearing two *N*-$CH_2COC_6H_5$ groups has been prepared by the reaction of 3,14-dimethyl-2,6,13,17-tetraazatricyclo$[16.4.0.0^{7.12}]$docosane (L^1) with phenacyl bromide. Interestingly, H_2L^2 reacts with Ni^{2+} ion to form two geometric isomers, *trans*-$[Ni(H_2L^2)]^{2+}$ and *cis*-$[Ni(H_2L^2)]^{2+}$. The axial Ni–O (*N*-$CH_2COC_6H_5$ group) bond distance (2.080(2) Å) of *trans*-$[Ni(H_2L^2)](ClO_4)_2 \cdot 2DMSO$ is shorter than the in-plane Ni–N distances (2.096(2) and 2.100(2) Å). However, the Ni–O distances (2.105(2) and 2.124(2) Å) of *cis*-$[Ni(H_2L^2)](ClO_4)_2 \cdot H_2O$ are considerably longer than the Ni–N distances (2.053(2)–2.086(2) Å). Each *N*-$CH_2COC_6H_5$ group of *trans*-$[Ni(H_2L^2)]^{2+}$ and *cis*-$[Ni(H_2L^2)]^{2+}$ exists as its *keto* form in the solid state and in various solvents. Two *N*-$CH_2COC_6H_5$ groups of *trans*-$[Ni(H_2L^2)]^{2+}$ are readily deprotonated in basic aqueous solutions, producing the *enolate* form *trans*-$[Ni(L^2)]$. On the other hand, *cis*-$[Ni(H_2L^2)]^{2+}$ undergoes deprotonation to yield *cis*-$[Ni(HL^2)]^{+}$, in which one *N*-$CH_2COC_6H_5$ group is not deprotonated, under similar conditions.

1. Introduction

Polyaza macrocyclic ligands and complexes bearing additional functional pendant arms have received much attention because of their interesting chemical properties and potential applications in various fields [1–16]. In general, coordination polyhedron and chemical properties of such complexes are influenced by the nature of the functional groups. Furthermore, chemical properties of the functional groups attached to a coordinated macrocycle are also influenced by the nature of the central metal ion and, therefore, are often quite different from those attached to a metal-free organic compound [11–14].

Various types of functionalized macrocyclic compounds have been prepared and investigated. Some polyaza macrocycles bearing *N*-COC_6H_5 pendant arms, such as L^6, have also been reported [15,16]. However, relatively few studies have been devoted to the synthesis of tetraaza macrocyclic complexes bearing ketone groups (*N*-$(CH_2)_n$COR). As far as we know, the preparation of 14-membered tetraaza macrocycles bearing *N*-$CH_2COC_6H_5$ pendant arms has not been reported.

In this work, we prepared a new 14-membered tetraaza macrocycle H_2L^2 bearing two *N*-$CH_2COC_6H_5$ pendant arms. Interestingly, H_2L^2 reacts with nickel(II) ion to form both *cis*-$[Ni(H_2L^2)]^{2+}$ and *trans*-$[Ni(H_2L^2)]^{2+}$ that are readily deprotonated to *cis*-$[Ni(HL^2)]^{+}$ and *trans*-$[Ni(L^2)]$, respectively, in basic conditions. Synthesis and characterization of the nickel(II) complexes are reported, together with crystal structures of *cis*- and *trans*-$[Ni(H_2L^2)](ClO_4)_2$. The formation of *cis*-$[Ni(H_2L^2)]^{2+}$ as well as the *trans* isomer in the present work is interesting, because most other related macrocycles bearing two *N*-functional pendant arms, such as L^3, L^4, and L^5, are reported to form only *trans*-octahedral nickel(II) complexes [8–10].

2. Experimental

2.1. Measurements

Electronic absorption spectra were recorded with an Analytic Jena Specord 200 UV–Vis spectrophotometer, infrared spectra with a Genesis II FT-IR spectrometer, NMR spectra with a Varian Mercury 300 FT NMR spectrometer, and GC–mass spectra with a Shimadzu a Z18 Oyster Conductivity/Temperature meter GCMSD-QP5050 spectrometer. Conductance measurements were taken with a Z18 Oyster Conductivity/Temperature meter. Magnetic moments were calculated from magnetic susceptibility data obtained at 293 K using a Johnson Matthey MK-1 magnetic susceptibility balance.

---

* Corresponding author. Tel.: +82 53 850 6443; fax: +82 53 850 6449.
E-mail address: sgkang@daegu.ac.kr (S.-G. Kang).

0020-1693/$ - see front matter © 2012 Elsevier B.V. All rights reserved.
http://dx.doi.org/10.1016/j.ica.2012.02.026

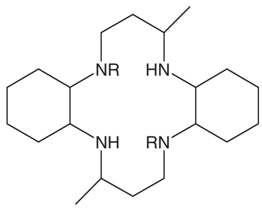

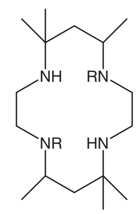

L^1: R = H

L^6: R = Y

L^2: R = X

L^3: R = CH_2CH_2OH

L^4: R = CH_2CONH_2

L^5: R = CH_2CH_2COOMe

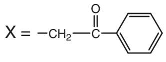

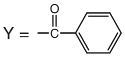

Molar susceptibilities were corrected for diamagnetism of the ligand and/or the anions by use of Pascal's constants. Elemental analyses were performed at the Research Center for Instrumental Analysis, Daegu University, Gyeongsan, Korea. FAB-mass spectra were performed at the Korea Basic Science Institute, Daegu, Korea.

2.2. Preparation of H_2L^2

The macrocycle L^1 was prepared by the reported procedure [17]. A chloroform solution (30 ml) of L^1 (2.0 g, 6.0 mmol) and phenacyl bromide (3.5 g, 17.6 mmol) was refluxed for *ca.* 30 h and then stored in a refrigerator until a white precipitate formed. The solid collected by filtration was dissolved in acetonitrile (20 ml). After the addition of 1.0 M NaOH aqueous solution (20 ml), the mixture was evaporated at room temperature to precipitate a white solid. It was collected by filtration and was recrystallized from warm chloroform–methanol (3:1) solution. Yield: ~70%. *Anal.* Calc. for $C_{36}H_{52}N_4O_2$ (Mw: 572.8): C, 75.48; H, 9.15; N, 9.78. Found: C, 75.10; H, 8.82; N, 9.94%. GC–mass (*m*/*z*): 573 (M^+). IR (cm^{-1}): 3298(ν_{N-H}), 1637($\nu_{C=O}$). ^1H NMR ($CDCl_3$): δ 1.03 (*d*, Me), 7.2 (*d*, C_6H_5), 7.3 (*d*, C_6H_5), 7.6 (*d*, C_6H_5). ^{13}C NMR ($CDCl_3$): 18.0, 21.5, 25.0, 25.6, 29.7, 34.2, 48.5, 50.8, 56.1, 77.5, 106.5, 125.2, 127.3, 127.7, 128.2, 128.9, 129.6, 138.3 ($-CH_2COC_6H_5$) ppm.

2.3. Preparation of $[H_4L^2](ClO_4)_2$

To an acetonitrile suspension (20 ml) of H_2L^2 (1.0 g) was added concentrated $HClO_4$ (1.0 ml) dissolved in water (20 ml). The mixture was stirred for 1 h at room temperature. The white solid, which had been formed, was collected by filtration, washed with water, and dried in air. Yield: ~90%. *Anal.* Calc. for $C_{36}H_{54}Cl_2N_4O_{10}$: C, 55.88; H, 7.03; N, 7.24. Found: C, 55.52; H, 6.95; N, 7.37%. FAB mass (*m*/*z*): 673.4 for $[H_4L^2+ClO_4]^+$, 573.5 for $[H_3L^2]^+$. IR (cm^{-1}): 3230(ν_{N-H}), 1640 ($\nu_{C=O}$), 1100 (ν_{Cl-O}, ClO_4^-).

2.4. Preparation of *trans*-$[Ni(H_2L^2)](ClO_4)_2$

To a boiling methanol solution (30 ml) of H_2L^2 (0.5 g) was added $Ni(OAc)_2{\cdot}4H_2O$ (*ca.* 2.0 g). The mixture was refluxed for 1 h and then cooled to room temperature. After the addition of $HClO_4$ (2.0 ml) and water (10 ml), the resulting solution was allowed to stand at room temperature to produce a pale yellow solid. The product was collected by filtration, washed with methanol, and dried in air. The crude product contains relatively small amount (<20%) of an orange solid {*cis*-$[Ni(H_2L^2)](ClO_4)_2$}. The solubility of *trans*-$[Ni(H_2L^2)](ClO_4)_2$ in acetonitrile–water (3:1) was found to be considerably higher than that of *cis*-$[Ni(H_2L^2)](ClO_4)_2$. The pure product was isolated by fractional recrystallizations of the crude product in acetonitrile–water (3:1). Yield: ~60%. *Anal.* Calc. for $C_{36}H_{52}Cl_2N_4NiO_{10}$ (Mw: 830.42): C, 52.07; H, 6.31; N, 6.75. Found: C, 51.74; H, 6.16; N, 6.48%. FAB mass (*m*/*z*): 729.4 for $[Ni(H_2L^2)+ClO_4]^+$, 629.5 for $[Ni(HL^2)]^+$. IR (cm^{-1}): 3223 (ν_{N-H}), 1631 ($\nu_{C=O}$), 1100 (ν_{Cl-O}, ClO_4^-). Magnetic moment (μ_{eff}): 2.90 μ_B at 20 °C.

2.5. Preparation of *cis*-$[Ni\ (H_2L^2)](ClO_4)_2$

To a boiling methanol solution (30 ml) of $Ni(OAc)_2{\cdot}4H_2O$ (*ca.* 2.0 g) was added H_2L^2 (0.5 g). The mixture was refluxed for 1 h and then cooled to room temperature. After the addition of $HClO_4$ (2.0 ml) and water (10 ml), the resulting solution was allowed to stand at room temperature to produce an orange solid. The product was collected by filtration, washed with methanol, and dried in air. The crude product also contains relatively small amount (<20%) of a pale yellow solid {*trans*-$[Ni(H_2L^2)](ClO_4)_2$}. The pure product was isolated by the fractional recrystallizations of the crude product in acetonitrile–water (3:1). Yield: ~60%. *Anal.* Calc. for $C_{36}H_{52}Cl_2N_4NiO_{10}$ (Mw: 830.42): C, 52.07; H, 6.31; N, 6.75. Found: C, 52.28; H, 6.26; N, 6.74%. FAB mass (*m*/*z*): 729.4 for $[Ni(H^2L^2)+ClO_4]^+$, 629.5 for $[Ni(HL^2)]^+$. IR (cm^{-1}): 3217 (ν_{N-H}), 3261 (ν_{N-H}), 1660 ($\nu_{C=O}$), 1640 ($\nu_{C=O}$), 1100 (ν_{Cl-O}, ClO_4^-). Magnetic moment (μ_{eff}): 2.92 μ_B at 20 °C.

2.6. Preparation of *trans*-$[NiL^2]$

To an acetonitrile solution (20 ml) of *trans*-$[Ni(H_2L^2)](ClO_4)_2$ (0.5 g) was added 0.1 M NaOH aqueous solution (20 ml). The resulting solution was evaporated at room temperature to precipitate a pale purple solid. The product was collected by filtration, washed with water, and dried in air. It was recrystallized from chloroform. Yield: ~80%. *Anal.* Calc. for $C_{36}H_{50}N_4NiO_2$ (Mw: 629.5): C, 68.69; H, 8.01; N, 8.90. Found: C, 68.02; H, 7.83; N, 8.65%. FAB mass (*m*/*z*): 629.5 for $[Ni(HL^2)]^+$. IR (cm^{-1}): 3235 (ν_{N-H}). Magnetic moment (μ_{eff}): 2.88 μ_B at 20 °C.

2.7. Preparation of *cis*-$[Ni(HL^2)]ClO_4$

To an acetonitrile solution (20 ml) of *cis*-$[Ni(H_2L^2)](ClO_4)_2$ (0.5 g) was added 0.1 M NaOH aqueous solution (20 ml). The resulting solution was evaporated at room temperature to precipitate a pale orange solid. The product was collected by filtration, washed with water, and dried in air. It was recrystallized from methanol. Yield: ~80%. *Anal.* Calc. for $C_{36}H_{51}ClN_4NiO_6$ (Mw: 729.96): C, 59.23; H, 7.04; N, 7.68. Found: C, 59.03; H, 7.16; N, 7.26%. FAB mass (*m*/*z*): 729.6 for $[Ni(H_2L^2)+ClO_4]^+$, 629.7 for $[Ni(HL^2)]^+$. IR (cm^{-1}): 3240 (ν_{N-H}), 3268 (ν_{N-H}), 1660 ($\nu_{C=O}$), 1100 (ν_{Cl-O}, ClO_4^-). Magnetic moment (μ_{eff}): 2.85 μ_B at 20 °C.

2.8. Crystal structure determination

Single crystals of *trans*-$[Ni(H_2L^2)](ClO_4)_2{\cdot}2DMSO$ and *cis*-$[Ni(H_2L^2)](ClO_4)_2{\cdot}H_2O$ suitable for X-ray study were grown from water–DMSO and water–acetonitrile solutions, respectively. Intensity data were collected on a Rigaku R-AXIS RAPID II-S diffractometer equipped with graphite monochromated Mo Kα (λ = 0.71073 Å) radiation source and imaging plate detector (460 × 256 mm). A total of 240 oscillation images were collected at 100 k using widths of 3° in ω the raw data were processed to give structure factors using the RAPID AUTO program. The structure was solved

Table 1
Crystallographic data for *trans*-$[Ni(H_2L^2)](ClO_4)_2 \cdot 2DMSO$ and *cis*-$[Ni(H_2L^2)](ClO_4)_2 \cdot H_2O$.

Compound	*trans*-$[Ni(H_2L^2)](ClO_4)_2 \cdot 2DMSO$	*cis*-$[Ni(H_2L^2)](ClO_4)_2 \cdot H_2O$
Empirical formula (*M*)	$C_{40}H_{64}Cl_2N_4NiO_{12}S_2$ (986.68)	$C_{36}H_{54}Cl_2N_4NiO_{11}$ (848.50)
Crystal system (space group)	monoclinic ($P2_1/c$)	monoclinic ($P2_1/c$)
Unit cell dimensions		
a (Å)	12.042(2)	11.023(2)
b (Å)	10.330(2)	16.901(1)
c (Å)	18.148(2)	20.777(2)
Beta (°)	92.174(3)	96.373(2)
V ($Å^3$)	2255.7(4)	3846.8(4)
Z	2	4
D_{calc} ($g\ cm^{-3}$)	1.453	1.462
θ range for data collection (°)	2.99–27.44	3.04–27.44
F(000)	1044	1784
μ (mm^{-1})	0.706	7.08
T (K)	293(2)	293(2)
Index ranges	$-15 \leqslant h \leqslant 15$, $-13 \leqslant k \leqslant 13$, $-23 \leqslant l \leqslant 23$	$-11 \leqslant h \leqslant 14$, $-21 \leqslant k \leqslant 21$, $-26 \leqslant l \leqslant 26$
Independent reflections	5146	8786
Reflections observed (>2σ)	4063	6916
Data completeness	1.000	1.00
Data/restraints/parameters	5146/0/277	8786/0/482
Goodness-of-fit (GOF) on F^2	1.060	1.040
Final *R* indices [$I > 2\sigma(I)$]	$R_1 = 0.0615$, $wR_2 = 0.1752$	$R_1 = 0.0586$, $wR_2 = 0.1556$
R indices (all data)	$R_1 = 0.0767$, $wR_2 = 0.1922$	$R_1 = 0.0769$, $wR_2 = 0.1703$
Largest difference in peak and hole (e $Å^{-3}$)	0.795 and −0.955	1.160 and −0.600

by direct method and refined by full matrix least squares against F^2 for all data using SHELXL-97 [18]. All non-hydrogen atoms were anisotropically refined. All other hydrogen atoms were included in the calculated position. Experimental details for the structure determinations are listed in Table 1.

3. Results and discussion

3.1. Synthesis

The macrocycle H_2L^2 bearing two *N*-$CH_2COC_6H_5$ pendant arms was prepared by the reaction of L^1 with phenacyl bromide. The mass, ^1H NMR, ^{13}C NMR, and IR spectral data of H_2L^2 and/or $[H_4L^2](ClO_4)_2$ are listed in Section 2. The di-*N*-functionalized macrocycle is soluble in chloroform, but is nearly insoluble in methanol at room temperature.

The reaction of $Ni(OAc)_2 \cdot 4H_2O$ with H_2L^2 in methanol, followed by addition of $NaClO_4$ or $HClO_4$, produces a mixture of two geometric isomers, *cis*-$[Ni(H_2L^2)](ClO_4)_2$ and *trans*-$[Ni(H_2L^2)](ClO_4)_2$. Interestingly, the proportion of *cis*-$[Ni(H_2L^2)](ClO_4)_2$ to *trans*-$[Ni(H_2L^2)](ClO_4)_2$ in the product is dependent on the reaction conditions (see Section 2). The major product prepared by adding H_2L^2 to a boiling methanol solution of $Ni(OAc)_2 \cdot 4H_2O$ was the *trans* isomer. On the other hand, the *cis* isomer could be prepared as the major product by the addition of $Ni(OAc)_2 \cdot 4H_2O$ to a boiling methanol solution of H_2L^2. The addition of a base to an aqueous solution of *trans*-$[Ni(H_2L^2)](ClO_4)_2$ yields the *enolate* form *trans*-$[NiL^2]$, in which two functional pendant arms are deprotonated. However, the only complex isolated from basic aqueous solutions of *cis*-$[Ni(H_2L^2)](ClO_4)_2$ is *cis*-$[Ni(HL^2)]ClO_4$; one of the two pendant arms is not deprotonated. The deprotonation of the *N*-$CH_2COC_6H_5$ group attached to *cis*-$[Ni(HL^2)]ClO_4$ could not be achieved even in 1.0 M NaOH aqueous solution.

3.2. Crystal structure of trans-$[Ni(H_2L^2)](ClO_4)_2 \cdot 2DMSO$

The isomer *trans*-$[Ni(H_2L^2)]^{2+}$ has slightly distorted *trans*-octahedral coordination geometry; the axial positions are occupied by the oxygen atoms of the *N*-$CH_2COC_6H_5$ pendant arms (Fig. 1). The macrocycle adopts a *trans*-III type *N*-conformation, and the complex has an inversion center at the nickel atom. The six-membered chelate rings and the cyclohexane rings of the complex adopt stable chair conformations.

Selected bond distances and angles of *trans*-$[Ni(H_2L^2)]^{2+}$ are listed in Table 2. The Ni–N (2.095(2) and 2.097(3) Å) distances are comparable with those of other related *trans*-octahedral nickel(II) complexes, such as *trans*-$[NiL^3](ClO_4)_2$ and *trans*-$[NiL^4](ClO_4)_2$ [8,9]. One of the most remarkable structural features of the complex is that the axial Ni–O (*N*-$CH_2COC_6H_5$ group) distance (2.083(2) Å) is shorter than the in-plane Ni–N distances. The Ni–O distance is distinctly shorter than the axial Ni–O (pendant *N*-CH_2CH_2OH or *N*-CH_2CONH_2 group) distances of *trans*-$[NiL^3](ClO_4)_2$ (2.149(4) Å) and *trans*-$[NiL^4](ClO_4)_2$ (2.302(3) Å) [8,9]. This

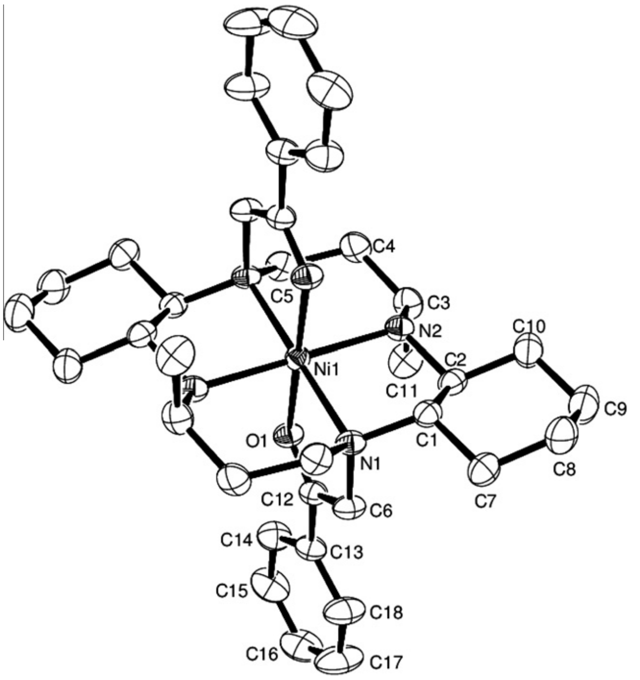

Fig. 1. An ORTEP drawing of symmetric unit of *trans*-$[Ni(H_2L^2)](ClO_4)_2 \cdot 2DMSO$ (symmetry code; −*x*, 1/2 + *y*, 1/2 − *z*). Lattice DMSO and perchlorate anions are omitted for clarity.

Table 2
Bond distances [Å] and angles [°] for *trans*-$[Ni(H_2L^2)](ClO_4)_2{\cdot}2DMSO$.

Ni(1)–N(1)	2.095(2)	Ni(1)–N(2)	2.097(3)
Ni(1)–O(1)	2.083(2)	C(11)–O(1)	1.234(4)
C(10)–C(11)	1.508(4)	C(11)–C(12)	1.483(4)
N(1)–Ni–N(2)	85.1(1)	N(1)–Ni–N(2)[a]	94.9(1)
N(1)–Ni–N(1)[a]	180.0(2)	N(2)–Ni–N(2)[a]	180.0(2)
N(1)–Ni–O(1)	81.5(2)	N(2)–Ni–O(1)	93.5(2)
O(1)–Ni–O(1)[a]	180.0(2)	C(10)–C(11)–O(1)	120.0(3)

[a] Symmetry code; 1 − *x*, 2 − *y*, −*z*.

indicates that the *N*-$CH_2COC_6H_5$ groups in *trans*-$[Ni(H_2L^2)]^{2+}$ bind the metal more strongly than those of the *N*-CH_2CH_2OH or *N*-CH_2CONH_2 groups in *trans*-$[NiL^3](ClO_4)_2$ and *trans*-$[NiL^4](ClO_4)_2$. The C(11)–O(1) distance (1.234(4) Å) is corresponding to the C=O double bond of a ketone group. The N(1)–Ni–N(2) angle (85.1(1)°) involved in the five-membered chelate ring is smaller than the N(1)–Ni–N(2)# angle (94.9(1)°) involved in the six-membered chelate ring, as usual. The Ni–O(1) bond is not perpendicular to the NiN_4 plane with N(1)–Ni–O(1) angle of 81.5(2)°. The C(10)–C(11)–O(1) angle is 120.0(3)°.

3.3. Crystal structure of cis-$[Ni(H_2L^2)](ClO_4)_2{\cdot}H_2O$

The ORTEP drawing (Fig. 2) of *cis*-$[Ni(H_2L^2)]^{2+}$ cation shows that the *N*-$CH_2COC_6H_5$ pendant arms as well as the four nitrogen atoms are involved in coordination. In contrast to *trans*-$[Ni(H_2L^2)]^{2+}$, the ketone groups in this isomer are *cis* to each other. The macrocycle is folded along the N(1)–Ni–N(3) axis and adopts *cis*-II type *N*-conformation.

Selected bond distances and angles of *cis*-$[Ni(H_2L^2)]^{2+}$ are listed in Table 3. The Ni–N distances (2.053(2)–2.086(2) Å) are not quite different from the Ni–N distances of *trans*-$[Ni(H_2L^2)]^{2+}$. However, the Ni–O distances (2.105(2)–2.124(2) Å) of *cis*-$[Ni(H_2L^2)]^{2+}$ are distinctly longer than the Ni–N distances and are ⩾0.02 Å longer than those (2.083(2) Å) of *trans*-$[Ni(H_2L^2)]^{2+}$. The N(1)–Ni–N(3) angle (171.9(1)°) is slightly deviated from 180°. The N(2)–Ni–O(1) and N(4)–Ni–O(2) angles (171.9(1) and 169.4(1)°, respectively) are also deviated from 180°. The N(2)–Ni–N(4) angle (100.9(1)°) is even smaller than 120°, showing that the macrocycle is folded along the N(1)–Ni–N(3) axis. The N(1)–Ni–N(2) and N(3)–Ni–N(4) angles (95.8(1)–100.9(1)°) involved in the six-membered chelate rings are considerably larger than the N(1)–Ni–N(4) and N(2)–Ni–N(3) angles (86.4(1)°) involved in the five-membered chelate rings. The N(1)–Ni–O(1) and N(3)–Ni–O(2) angles (80.0(1)–81.6(1)°) are smaller than the N(1)–Ni–N(4) and N(2)–Ni–N(3) angles. It is also seen that the O(1)–Ni–O(2) angle (82.7(1)°) is much smaller than 90°. The C(19)–C(20)–O(1) angle is 118.6(3)°.

Table 3
Bond distances [Å] and angles [°] for *cis*-$[Ni(H_2L^2)](ClO_4)_2{\cdot}H_2O$.

Ni(1)–N(1)	2.065(2)	Ni(1)–N(2)	2.075(2)
Ni(1)–N(3)	2.053(2)	Ni(1)–N(4)	2.086(2)
Ni(1)–O(1)	2.105(2)	Ni(1)–O(2)	2.124(2)
C(20)–O(1)	1.230(4)	C(28)–O(2)	1.234(3)
C(19)–C(20)	1.524(4)	C(20)–C(21)	1.483(4)
C(27)–C(28)	1.511(4)	C(28)–C(29)	1.482(4)
N(1)–Ni–N(2)	100.9(1)	N(1)–Ni–N(3)	171.9(1)
N(1)–Ni–N(4)	86.4(1)	N(2)–Ni–N(3)	86.4(1)
N(2)–Ni–N(4)	100.9(1)	N(3)–Ni–N(4)	95.8(1)
N(1)–Ni–O(1)	80.0(1)	N(1)–Ni–O(2)	94.9(1)
N(2)–Ni–O(1)	171.9(1)	N(2)–Ni–O(2)	89.3(1)
N(3)–Ni–O(1)	92.3(1)	N(3)–Ni–O(2)	81.6(1)
N(4)–Ni–O(1)	87.2(1)	N(4)–Ni–O(2)	169.4(1)
O(1)–Ni–O(2)	82.7(1)	C(1)–N(1)–C(18)	115.6(1)
C(9)–N(3)–C(10)	113.0(2)	O(1)–C(20)–C(19)	118.6(3)

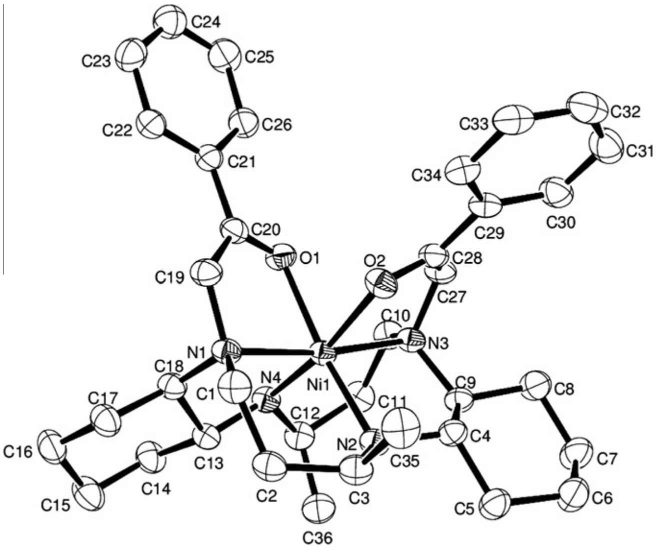

Fig. 2. An ORTEP drawing of symmetric unit of *cis*-$[Ni(H_2L^2)](ClO_4)_2{\cdot}H_2O$. Lattice water and perchlorate anions are omitted for clarity.

3.4. Spectra and properties of trans-$[Ni(H_2L^2)](ClO_4)_2$ and trans-$[Ni(L^2)]$

As described above, the coordinated *N*-$CH_2COC_6H_5$ groups in *trans*-$[Ni(H_2L^2)]^{2+}$ are readily deprotonated in basic aqueous solutions, yielding *trans*-$[Ni(L^2)]$ bearing two *N*-$CH{=}C(O^-)C_6H_5$ groups that are protonated in acidic solutions (Eq. (1)). However, both *trans*-$[Ni(H_2L^2)](ClO_4)_2$ and *trans*-$[Ni(L^2)]$ are quite stable in the solid states or in various pure solvents.

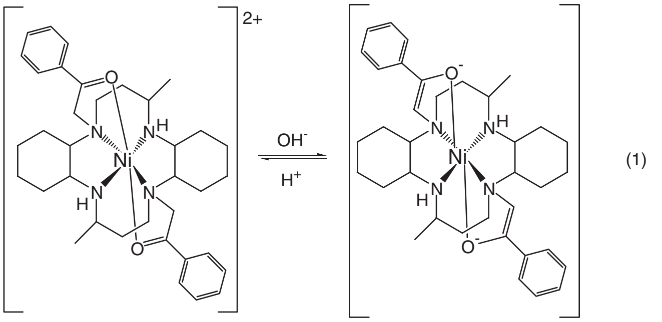

(1)

The complex *trans*-$[Ni(H_2L^2)](ClO_4)_2$ is soluble in acetonitrile and nitromethane. On the other hand, *trans*-$[Ni(L^2)]$ is soluble in chloroform, but is nearly insoluble in acetonitrile or nitromethane. The values of molar conductance (Table 4) for *trans*-$[Ni(H_2L^2)](ClO_4)_2$ measured in nitromethane (148 Ω^{-1} mol^{-1} cm^2) and acetonitrile (260 Ω^{-1} mol^{-1} cm^2) indicate that the complex is a 1:2 electrolyte. The *enolate* form *trans*-$[Ni(L^2)]$ was found to be a non-electrolyte in chloroform. FAB mass spectrum of *trans*-$[Ni(H_2L^2)](ClO_4)_2$ shows two groups of peaks at *m*/*z* 729.4 {$[Ni(H_2L^2)+ClO_4]^+$} and 629.5 {$[Ni(HL^2)]^+$}. The spectrum of *trans*-$[Ni(L^2)]$ shows a peak at *m*/*z* 629.5. The magnetic moments of *trans*-$[Ni(H_2L^2)](ClO_4)_2$ and *trans*-$[Ni(L^2)]$ in the solid states were found to be 2.90 and 2.88 μ_B, respectively, at room temperature, showing the d^8 electronic configuration of octahedral geometry. The IR spectrum of *trans*-$[Ni(H_2L^2)](ClO_4)_2$ shows $\nu_{C=O}$ of the coordinated *N*-$CH_2COC_6H_5$

Table 4
Molar conductance and electronic absorption spectral data of the nickel(II) complexes.

Complex	λ_{max}, nm[a] (ε, M^{-1} cm^{-1})		λ_M, Ω^{-1} mol^{-1} cm^2
trans-$[Ni(H_2L^2)](ClO_4)_2$	594(3.3)	735(3.2)	140 260[b]
	605(3.5)[b]	740(3.6)[b]	60[c]
	585(3.3)[c]	732(3.3)[c]	
trans-$[NiL^2]$	570(6.4)[d]	805(3.6)[d]	0[d]
cis-$[Ni(H_2L^2)](ClO_4)_2$	511(56)	825(16)	135 245[b]
	515(57)[b]	830(16)[b]	55[c]
	517(60)[c]	845(18)[c]	
cis-$[Ni(HL^2)]ClO_4$	505(sh)	805(11)	60 90[b]
	525(sh)[b]	795(10)[b]	
trans-$[NiL^3](ClO_4)_2$[e]	516(7.2)		
trans-$[NiL^4](ClO_4)_2$[f]	525(6.9)		

[a] Measured in nitromethane at 20 °C unless otherwise specified.
[b] In acetonitrile.
[c] In DMSO.
[d] In chloroform.
[e] Ref. [8].
[f] Ref. [9].

groups at 1631 cm^{-1}. A band corresponding to ν_{N-H} of the secondary amino groups is observed at 3223 cm^{-1}. In the spectrum of *trans*-$[Ni(L^2)]$, ν_{N-H} of the secondary amino groups is observed at 3235 cm^{-1}; however, no peak corresponding to $\nu_{C=O}$ was observed.

The electronic absorption spectra (Table 3) of *trans*-$[Ni(H_2L^2)](ClO_4)_2$ measured in various solvents show d–d transition bands around 600 (ε = 3.3–3.5 M^{-1} cm^{-1}) and 735 nm (ε = 3.2–3.6 M^{-1} cm^{-1}). The spectra are quite different from those of various other related *trans*-octahedral nickel(II) complexes, such as *trans*-$[NiL^3](ClO_4)_2$ [8] and *trans*-$[NiL^4](ClO_4)_2$ [9]; one (*ca.* 600 nm) of the bands is observed at >60 nm longer wavelength than that of *trans*-$[NiL^3](ClO_4)_2$ (516 nm) or *trans*-$[NiL^4](ClO_4)_2$ (525 nm). The spectrum of *trans*-$[Ni(L^2)]$ measured in chloroform exhibits the bands at 570 (ε = 3.3 M^{-1} cm^{-1}) and 805 nm (ε = 3.6 M^{-1} cm^{-1}) that are somewhat shorter and considerably longer, respectively, than those for *trans*-$[Ni(H_2L^2)](ClO_4)_2$.

3.5. Spectra and properties of cis-$[Ni(H_2L^2)](ClO_4)_2$ and cis-$[Ni(HL^2)]ClO_4$

The *cis* isomer *cis*-$[Ni(H_2L^2)]^{2+}$ also undergoes deprotonation in basic aqueous solutions. However, the only complex isolated from the solutions is *cis*-$[Ni(HL^2)]^+$ where one of the two pendant arms is not deprotonated (Eq. (2)). This deprotonation behavior is quite different from the behavior of *trans*-$[Ni(H_2L^2)]^{2+}$. The deprotonation of the free macrocycle H_2L^2 was also attempted in 0.1–3.0 M NaOH aqueous solutions, but failed; the only compound isolated from the solutions was found to be H_2L^2. As mentioned above, the Ni–O interactions of the *cis* isomer are weaker than those of the *trans* isomer. Therefore, it can be suggested that the difference in the deprotonation behaviors between the two isomers is closely related to the Ni–O interactions; the stronger the Ni–O interactions, the easer the deprotonation of the *N*-$CH_2COC_6H_5$ group.

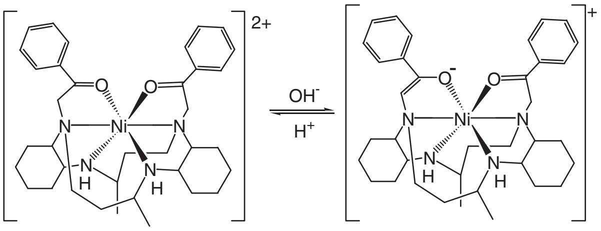

(2)

Both *cis*-$[Ni(H_2L^2)](ClO_4)_2$ and *cis*-$[Ni(HL^2)]ClO_4$ are soluble in acetonitrile and nitromethane. The complexes are quite stable in the solid states and in various solvents. The values of molar conductance (Table 3) for *cis*-$[Ni(H_2L^2)](ClO_4)_2$ and *cis*-$[Ni(HL^2)]ClO_4$ measured in nitromethane or acetonitrile show that they are 1:2 and 1:1 electrolytes, respectively. FAB mass spectrum of *cis*-$[Ni(H_2L^2)](ClO_4)_2$ is nearly identical with that of *trans*-$[Ni(H_2L^2)](ClO_4)_2$. The spectrum of *cis*-$[Ni(HL^2)]ClO_4$ shows two groups of peaks at *m*/*z* 729.6 and 629.7. The magnetic moments of *cis*-$[Ni(H_2L^2)](ClO_4)_2$ (2.92 μ_B) and *cis*-$[Ni(HL^2)]ClO_4$ (2.85 μ_B) measured in the solid states also support the fact that the complexes have octahedral coordination geometry. The IR spectrum of *cis*-$[Ni(H_2L^2)](ClO_4)_2$ shows ν_{N-H} of the secondary amino groups at 3261 and 3217 cm^{-1}. The spectrum also shows two bands corresponding to $\nu_{C=O}$ of the coordinated *N*-$CH_2COC_6H_5$ groups at 1640 and 1660 cm^{-1}. In the spectrum of *cis*-$[Ni(HL^2)]ClO_4$, one peak corresponding to $\nu_{C=O}$ of the coordinated *N*-$CH_2COC_6H_5$ group is observed at 1660 cm^{-1}. Two peaks of ν_{N-H} are also observed at 3268 and 3240 cm^{-1}. The electronic absorption spectrum of *cis*-$[Ni(H_2L^2)](ClO_4)_2$ measured in nitromethane shows the d–d transition bands at 511 (ε = 56 M^{-1} cm^{-1}) and 825 nm (ε = 16 M^{-1} cm^{-1}), which are comparable with those of other related octahedral nickel(II) complexes. The wavelengths of the d–d transition bands are quite different from those of *trans*-$[Ni(H_2L^2)](ClO_4)_2$. Furthermore, the molar absorption coefficient of each band for the *cis* isomer is distinctly larger than that of the *trans* isomer. The spectrum of *cis*-$[Ni(HL^2)]ClO_4$ is not quite different from that of *cis*-$[Ni(H_2L^2)](ClO_4)_2$.

4. Concluding remarks

This work shows that H_2L^2 bearing two *N*-$CH_2COC_6H_5$ pendant arms reacts with Ni^{2+} ion to form *cis*-$[Ni(H_2L^2)]^{2+}$ as well as *trans*-$[Ni(H_2L^2)]^{2+}$. To our knowledge, *cis*-$[Ni(H_2L^2)]^{2+}$ is a very rare example of 14-membered tetraaza macrocyclic nickel(II) complex with two *N*-functional pendant arms that occupy *cis* positions of the octahedron; L^3, L^4, and L^5 react with Ni^{2+} ion to form only *trans*-octahedral complexes [8–10]. The Ni–O (*N*-$CH_2COC_6H_5$ groups) bonds of *trans*-$[Ni(H_2L^2)]^{2+}$ are distinctly stronger than those of *cis*-$[Ni(H_2L^2)]^{2+}$. The *N*-$CH_2COC_6H_5$ groups in *trans*-$[Ni(H_2L^2)]^{2+}$ are readily deprotonated in basic aqueous solutions. On the other hand, one of the *N*-$CH_2COC_6H_5$ groups in *cis*-$[Ni(H_2L^2)]^{2+}$ does not undergo deprotonation under similar experimental conditions. This may be attributed to the relatively weak Ni–O interaction in the *cis* isomer.

Acknowledgments

This research was supported in part by Basic Science Research Program through the National Research Foundation of Korea (NRF) funded by the Ministry of Education, Science and Technology (No. 2010-0007251). C.-H. Kwak thanks Non-Directional Fund of Sunchon National University, 2011.

Appendix A. Supplementary material

Supplementary material CCDC 846198 and 846199 contains the supplementary crystallographic data for *cis*-[$Ni(H_2L^2)](ClO_4)_2\cdot H_2O$ and *trans*-[$Ni(H_2L^2)](ClO_4)_2\cdot 2DMSO$. These data can be obtained free of charge from The Cambridge Crystallographic Data Centre via www.ccdc.cam.ac.uk/data_request/cif. Supplementary data associated with this article can be found, in the online version, at http://dx.doi.org/10.1016/j.ica.2012.02.026.

References

[1] R.E. Mewis, S.J. Archibald, Coord. Chem. Rev. 254 (2010) 1686.
[2] N. Viola-Villegas, R.P. Doyle, Coord. Chem. Rev. 253 (2009) 1906.

[3] S.J. Archibald, Annu. Rep. Prog. Chem., Sect. A 106 (2010) 295.
[4] I. Lukes, J. Kotek, P. Vojtisek, P. Hermann, Coord. Chem. Rev. 216–217 (2001) 287.
[5] E.K. Barefield, Coord. Chem. Rev. 254 (2010) 1607.
[6] J. Costamagna, G. Ferraudi, B. Matsuhiro, M. Vampus-Vallette, J. Canales, M. Villagran, J. Vargas, M.J. Aguirre, Coord. Chem. Rev. 196 (2000) 125.
[7] V.G. Organo, A.S. Filatov, J.S. Quartararo, Z.M. Friedman, E.V. Rybak-Akimova, Inorg. Chem. 48 (2009) 8458.
[8] S.-G. Kang, M.-S. Kim, J.-S. Choi, D. Whag, K. Kim, J. Chem. Soc., Dalton Trans. (1995) 363.
[9] K.Y. Choi, H.-H. Lee, B.-B. Park, J.H. Kim, M.-W. Kim, J.-W. Ryu, M. Suh, I.-H. Suh, Polyhedron 20 (2001) 2002.
[10] S.-G. Kang, J.K. Kweon, J.H. Jeong, Inorg. Chim. Acta 360 (2007) 1875.
[11] L. Siegfried, A. Comparone, M. Neuburger, T.A. Kaden, Dalton Trans. (2005) 30.
[12] T.A. Kaden, Chimica 54 (2000) 574.
[13] S.-G. Kang, H. Kim, N. Kim, K. Nam, U. Lee, Inorg. Chim. Acta 363 (2010) 1694.
[14] S.-G. Kang, N. Kim, J.H. Jeong, Inorg. Chim. Acta 366 (2011) 247.
[15] C. Nirmala, A.K. Rahimanm, S. Sreedaran, R. Jegadeesh, N. Raaman, V. Narayanan, J. Mol. Struct. 989 (2011) 91.
[16] C. Nirmala, A.K. Rahimanm, S. Sreedaran, R. Jegadeesh, N. Raaman, V. Narayanan, Spectrochim. Acta Part A 77 (2010) 92.
[17] S.-G. Kang, J.K. Kweon, S.-K. Jung, Bull. Korean Chem. Soc. 12 (1991) 483.
[18] G.M. Sheldrick, Acta Crystallogr. A64 (2008) 112.